JACS
JOURNAL OF THE AMERICAN CHEMICAL SOCIETY

COMMUNICATION

pubs.acs.org/JACS

Stable Radical Anions Inside Fullerene Cages: Formation of Reversible Electron Transfer Systems

Takahiro Tsuchiya,[†] Mateusz Wielopolski,[‡] Noriko Sakuma,[†] Naomi Mizorogi,[†] Takeshi Akasaka,*[,†] Tatsuhisa Kato,[§] Dirk M. Guldi,[‡] and Shigeru Nagase[∥]

[†]Center for Tsukuba Advanced Research Alliance, University of Tsukuba, Tsukuba, Ibaraki 305-8577, Japan

[‡]Department of Chemistry and Pharmacy & Interdisciplinary Center for Molecular Materials (ICMM), Friedrich-Alexander-Universität Erlangen-Nürnberg, Egerlandstrasse 3, 91058 Erlangen, Germany

[§]Institute for the Promotion of Excellence in Higher Education, Kyoto University, Yoshida, Sakyo-ku, Kyoto 606-8501, Japan

[∥]Department of Theoretical Molecular Science, Institute for Molecular Science, Okazaki, Aichi 444-8585, Japan

Supporting Information

ABSTRACT: The complexation behavior of $La_2@C_{80}$ dimetallofullerenes with organic donor molecules (**D**) in solution has been investigated. It has been shown that $La_2@C_{80}$ and **D** form 1:1 complexes as a result of electron transfer interactions in the ground state. The equilibrium between $La_2@C_{80}$/**D** and $[La_2@C_{80}]^{\bullet-}/[\mathbf{D}]^{+}$ in solution is readily controlled by changing the temperature and solvent.

In recent years, a tremendous variety of supramolecular electron donor−acceptor systems based on fullerenes have been established.[1] Considering, for example, empty fullerenes, they exhibit all the hallmarks that are found in nature's highly sophisticated solar energy conversion/storage systems, namely, photosynthetic organisms in plants, algae, and in various types of bacteria.[2] Owing to its rigid structure, C_{60} possesses exceptionally small reorganization energies in charge transfer reactions, and features outstanding electron accepting properties. To this date, a myriad of systems, which exhibit efficient charge transfer between organic donors and C_{60}, have been reported.[3] Charge transfer evolves, however, in most of these systems from a photoexcited state, while ground state charge transfer is rather unusual. In this regard, endohedral metallofullerenes have attracted special attention due to their unique electronic properties and reactivities. Their properties differ strikingly from those known for empty fullerenes.[4] Among the endohedral metallofullerenes, lanthanum encapsulating systems are particularly interesting—they give rise to much lower reduction potentials than pristine fullerenes. The latter is one of the key parameters for controlling the reactivities of metallofullerenes.[5]

Recently, we have reported on the complexation behavior of paramagnetic endohedral metallofullerene $La@C_{2v}$-C_{82} with aza- and thiacrown ethers and organic donors in solution.[6] The binding affinities were found to be much stronger than those for C_{60}. Interestingly, complexation of $La@C_{82}$ induces ground state electron transfer—entirely without photoirradiation. In addition, it has been demonstrated that metallofullerenes comprising I_h-C_{80} cages [i.e., $M_3N@C_{80}$ (M = Sc[7] and Lu[8]) or $M_2@C_{80}$ (M = La[9] and Ce[10])] are promising materials for the design of electron donor−acceptor conjugates and hybrids suitable for the use in optoelectronic devices at the nanometer scale. Among these, $M_2@C_{80}$ reveal remarkably small band gaps. Exceptional are also their electron accepting properties. The reduction potential, on the other hand, is even higher than that of $La@C_{82}$.[11]

In this paper, we have examined the intermolecular complexation and electron transfer behavior between $La_2@C_{80}$ and organic donor molecules such as TMPD (Scheme 1). Our experimental assays have been complemented by theoretical calculations, which bring to light the complex electronic properties of the radical anion species of $La_2@C_{80}$.

The complexation behavior of $La_2@C_{80}$ with TMPD in nitrobenzene at room temperature was followed by standard titration techniques using vis-NIR spectroscopy. Figure 1 shows the evolution of the characteristic absorptions of the $[TMPD]^{\bullet+}$ radical cation at 568 and 620 nm[6a] upon increasing concentration of TMPD. In addition, in the NIR region, the appearance of a new low-intensity absorption band at 1160 nm and two isosbestic points at 670 and 990 nm is discernible. Notable, the 1160 nm maximum resembles the signature of the one-electron reduced form of C_{60}, as, for example, produced by flash photolysis, at 1070 nm[12] and those of $Sc_3N@C_{80}$, $Lu_3N@C_{80}$, $La_2@C_{80}$, and $Ce_2@C_{80}$ with maxima at 1120,[7a] 1025,[8] 1200,[9] and 900−1200 nm,[10] respectively. Hence, the absorption titration experiments in nitrobenzene suggest the successful formation of a ground-state electron transfer complex to yield $[La_2@C_{80}]^{\bullet-}/[TMPD]^{\bullet+}$.

To explore the excited state properties of $[La_2@C_{80}]^{\bullet-}/[TMPD]^{\bullet+}$ and to correlate them with the spectroscopic results on the complex formation, time-dependent density functional theory (TDDFT) methods have been employed, see Supporting Information for details. Figure 2 shows the resulting electronic configuration of $[La_2@C_{80}]^{\bullet-}$ as compared to $[Sc_3N@C_{80}]^{\bullet-}$ and $[C_{60}]^{\bullet-}$. Notable here is that the SOMO of $[La_2@C_{80}]^{\bullet-}$ exhibits the lowest energy among all of the occupied molecular orbitals.

For the spectroscopic discussion, we may consider the five energetically lowest excited states of the anion species of $La_2@C_{80}$ as calculated by TDDFT methods. The first three low-energy excitations are attributed to the excitation of one electron from the SOMO to three different unoccupied orbitals

Received: June 10, 2011
Published: July 18, 2011

dx.doi.org/10.1021/ja205391v | J. Am. Chem. Soc. 2011, 133, 13280–13283

Scheme 1

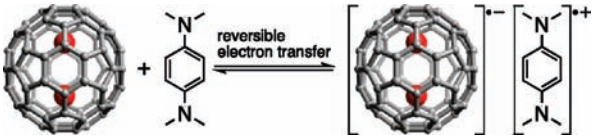

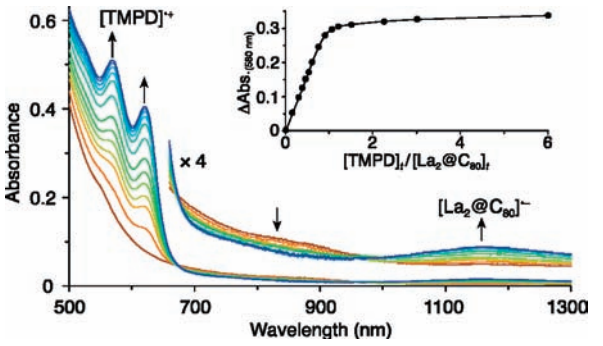

Figure 1. Vis-NIR spectra of $La_2@C_{80}$ (3.5×10^{-5} M) in the presence of TMPD (0−6 equiv) in nitrobenzene. Inset: titration plots at 580 nm.

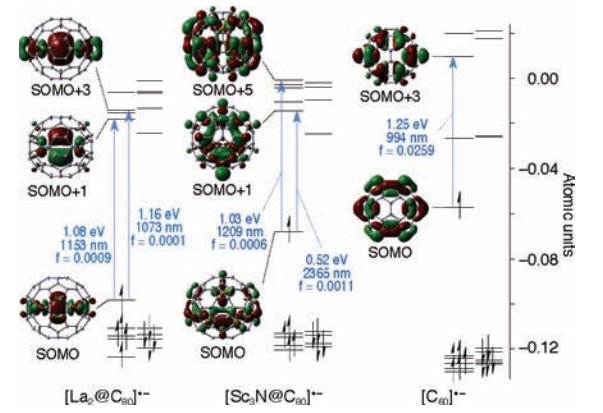

Figure 2. MO diagrams of $[La_2@C_{80}]^{\bullet-}$, $[Sc_3N@C_{80}]^{\bullet-}$, and $[C_{60}]^{\bullet-}$.

(SOMO+1 to SOMO+3). The two most dominant excited states refer to excitations into the orbitals SOMO+1 and SOMO+3, which are localized between the La atoms. All other excitations occur into orbitals that evolve from the mixing of the $\{La_2\}^{6+}$ and $\{C_{80}\}^{6-}$ states. The first excited state comprises the highest oscillator strength and leads to the most dominant but rather weak absorption. According to the calculations, this absorption is centered at 1153 nm (1.08 eV) and corresponds to the excitation of the additional electron within the La atoms of the reduced $La_2@C_{80}$ ($[La_2@C_{80}]^{\bullet-}$). Hence, our TDDFT computations nicely corroborate the spectroscopic investigations. The newly developing weak absorption maximum at 1160 nm upon complexation with TMPD clearly attests the successful formation of the one-electron reduced form of $La_2@C_{80}$ and the corresponding excitation of the additional electron into the SOMO. However, owing to the very low oscillator strength ($f = 0.0009$), its intensity is very weak. Considering the fact that the low-energy excited states infer excitations within La orbitals inside the cage, one may envision stabilizing and shielding effects of the C_{80} cavity. All of the remaining excitations (i.e., at higher energies) do not contribute to the absorption features of the one-electron reduced form of $La_2@C_{80}$ due to zero oscillator strengths. Notable, the singlet−singlet transitions of $[C_{60}]^{\bullet-}$ and $[Sc_3N@C_{80}]^{\bullet-}$ have been calculated to occur at 994 and 1209 nm, respectively (Figure 2). Thus, we believe that the features of the one-electron reduced form of $La_2@C_{80}$ fit perfectly in this context. The detailed orbital diagrams of neutral and radical anion species of $La_2@C_{80}$, $Sc_3N@C_{80}$, and C_{60} are illustrated in Figures S1−S4.[13] In general, it is rather difficult to distinguish between the neutral and the radical anion species of $La_2@C_{80}$ by means of steady-state absorption measurements. In both cases, the absorption cross sections are quite low and are located in similar regions of the spectrum, see Figure S5. Therefore, experimental results on the characteristic absorption wavelengths of the radical anion of $La_2@C_{80}$ have not been reported so far. However, our titration experiments unambiguously point to the reduction of $La_2@C_{80}$ due to the occurrence of the two isosbestic points. In conclusion, our theoretical investigations shed important light onto the characteristic absorption fingerprints of the one-electron reduced form of $La_2@C_{80}$.

Table 1. Oxidation Potentials ($^{ox}E_1$)[a] of the Donors and Thermodynamic Parameters for the Electron Transfer and the Binding between $La_2@C_{80}$ and Donors

compd	$^{ox}E_1$[b]	ΔG_{et}[c]	log K_{obs}	ΔG_{obs}[d]	$\Delta G_{obs} - \Delta G_{et}$	log K_{assoc}
TMPD	−0.30	−3.23	6.1	−8.25	−5.03	3.7
$FeCp^*_2$	−0.52	−8.30	6.9	−9.34	−1.04	0.8

[a] Obtained by CV in nitrobenzene at 296 K. [b] V vs Fc/Fc^+. [c] The driving forces for the electron transfer from organic donors to fullerenes. [d] The free-energy changes for the whole reaction, as obtained from the equation: ΔG_{obs} (kcal/mol) = $-RT \ln K_{obs}$.

Further, the titration plot in the inset of Figure 1 reveals an inflection point at the 1:1 ratio of $[La_2@C_{80}]$ to [TMPD], which is indicative for the formation of a 1:1 complex. This stoichiometry was also confirmed by supplementary Job's plot titration experiments (Figure S6). The binding constant for the $La_2@C_{80}$/TMPD system as evaluated by nonlinear least-squares curve fitting of the titration plots, was determined to log K_{obs} = 6.1. Importantly, this value is dependent on the solvent with binding constants of log K_{obs} = 5.7 and 4.5 in benzonitrile and *o*-dichlorobenzene, respectively. In toluene, on the other hand, the binding is too weak and, thus, hampers a meaningful analysis. Taking into account the different solvent permittivities ε_r, a stabilizing trend toward solvents with higher values of ε_r emerged. Such a trend agrees well with the fact that increasing the polarity of the solvent goes along with the stabilization of radical ion pairs.

In complementary experiments, the one-electron reduction of $La_2@C_{80}$ was confirmed using decamethylferrocene ($FeCp^*_2$) as electron donor (Figure S7). In this particular case, the higher binding constant of log K_{obs} = 6.9 correlates well with a lower first oxidation potential (Table 1).

Finally, the electron transfer in the $La_2@C_{80}$/TMPD system was probed in EPR measurements as summarized in Figure S8. The addition of $La_2@C_{80}$ to a nitrobenzene solution of TMPD evokes the appearance of an EPR signal due to $[TMPD]^{\bullet+}$. Its intensity is growing with the amount of $La_2@C_{80}$. The line width of the resulting EPR spectrum is as narrow as that of the $[TMPD]^{\bullet+}$ PF_6^- salt in solution, indicating that the stable spin is located on the time scale of the EPR experiment. Variable temperature EPR measurements from 320 to 260 K in

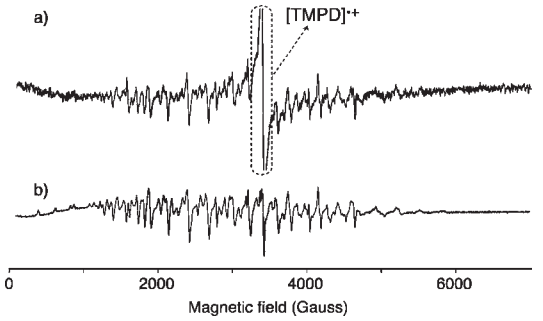

Figure 3. EPR spectra of (a) $La_2@C_{80}$ in the presence of 1 equiv of TMPD in nitrobenzene at 5 K ([TMPD] = 3.5×10^{-5} M) and (b) electrochemically generated radical anion of $La_2@C_{80}$ (n-BuN^+ $[La_2@C_{80}]^{\bullet-}$) at 2 K.

o-dichlorobenzene/benzonitrile (1:1 v/v) reveals that the equilibrium shifts to the formation of $[TMPD]^{\bullet+}$ at lower temperatures (Figure S9). Repeating the temperature variation affords the same spectra, denoting that the electron transfer from TMPD to $La_2@C_{80}$ is fully reversible. The EPR signal of $[La_2@C_{80}]^{\bullet-}$ was detected only under ultracold temperature conditions (Figure 3). Independent confirmation for this assignment came from reference experiments with n-Bu_4N^+ $[La_2@C_{80}]^{\bullet-}$[14] at 2 K. Here, the EPR spectrum reveals a very complex pattern ranging over 6000 gauss. The latter is due to the large hfc constant (~360 gauss) and relates to the large spin density between the two La atoms (Figure 3b). Meanwhile, EPR measurements of $La_2@C_{80}$ in the presence of TMPD at 5 K afforded spectra similar to those of the reference sample (Figure 3a).

Noteworthy, in absorption titration experiments with C_{60} and $Sc_3N@C_{80}$, on one hand, and TMPD, on the other hand, the appearance of the corresponding $[TMPD]^{\bullet+}$ absorption features evolved. However, the overall intensities were very weak and the equilibrium constants were too small to be determined. The thermodynamic driving forces for the electron transfer from TMPD to $Sc_3N@C_{80}$ and C_{60} are evaluated as 17.76 and 15.22 kcal/mol, respectively. In this context, we used the following relationship[15]

$$\Delta G_{et} = 23.06 \times [{}^{ox}E_1(donor) - {}^{red}E_1(fullerene)]$$

The corresponding values indicate a thermodynamically unfavorable electron transfer between TMPD and C_{60} as well as between TMPD and $Sc_3N@C_{80}$. In contrast, the low reduction potential of $La_2@C_{80}$ leads to a significant increase of the thermodynamic driving force and renders the electron transfer exothermic.[16] The ΔG_{et} values for $La_2@C_{80}$ are listed in Table 1. As a complement, the free-energy changes (ΔG_{obs}) were calculated from the aforementioned binding constants. A notable trend toward lower values emerged, with a disagreement that appears to be larger in the $La_2@C_{80}$/TMPD system. A likely rationale infers the fact that for the determination of ΔG_{et} in $La_2@C_{80}$/TMPD and in $La_2@C_{80}$/$FeCp^*_2$ neither different electron donor−acceptor separations nor different reorganization energies have been considered. However, it is obvious that a change in distance between $La_2@C_{80}$ and any of the electron donors will impact the electron transfer dynamics. Likewise, the association constants differ from those determined from the absorption titrations for $La_2@C_{80}$/TMPD and $La_2@C_{80}$/$FeCp^*_2$ with values of 3.7 and 0.8, respectively, when calculated via

$$\ln K_{assoc} = -(\Delta G_{obs} - \Delta G_{et})/RT$$

Steric hindrance of $FeCp^*_2$ is certainly one factor that is responsible for the small K_{assoc}. Overall, the bulky $FeCp^*_2$ ligand will adopt an unfavorable geometry within the otherwise stable complex with $La_2@C_{80}$.

In conclusion, it has been shown that $La_2@C_{80}$ reveals strong reversible intermolecular interactions with various organic donors. In solution, ground-state electron transfer was confirmed at complete equilibrium yielding stable radical ion complexes. The current work contrasts from previous investigations with paramagnetic $La@C_{82}$, in which the electron transfer is driven by the low LOMO level. The fact that even diamagnetic $La_2@C_{80}$ is susceptible toward ground-state electron transfer is interesting and relates to its exceptional LUMO orbital/level. Thus, we feel that the current results constitute an important milestone with respect to developing materials, which are suitable for modern electronic, magnetic, and optical applications. With enhancement of the longer wavelength absorption by using endohedral metallofullerene, improvement in the quantum efficiency and an increase in the current density of photovoltaics are also expected.

■ ASSOCIATED CONTENT

Supporting Information. Spectroscopic characterization data, details on theoretical calculations. This material is available free of charge via the Internet at http://pubs.acs.org.

■ AUTHOR INFORMATION

Corresponding Author
akasaka@tara.tsukuba.ac.jp

■ ACKNOWLEDGMENT

This work is supported in part by a Grant-in-Aid for Scientific Research on Innovative Areas (No. 20108001, "pi-Space"), a Grant-in-Aid for Scientific Research (A) (No. 20245006), a Grant-in-Aid for Young Scientists (B) (No. 22750030), The Next Generation Super Computing Project (Nanoscience Project), Nanotechnology Support Project, Grants-in-Aid for Scientific Research on Priority Area (Nos. 20036008, 20038007), and Specially Promoted Research (No. 22000009) from the Ministry of Education, Culture, Sports, Science, and Technology of Japan, The Strategic Japanese-Spanish Cooperative Program funded by JST and MICINN, and funding provided by the DFG (GU 517/11-1, SFB 583, and Cluster of Excellence Engineering of Advanced Materials).

■ REFERENCES

(1) (a) Hahn, U.; Cardinali, F.; Nierengarten, J.-F. *New J. Chem.* **2007**, *31*, 1128–1138. (b) Tashiro, K.; Aida, T. *Chem. Soc. Rev.* **2007**, *36*, 189–197. (c) Bonifazi, D.; Enger, O.; Diederich, F. *Chem. Soc. Rev.* **2007**, *36*, 390–414. (d) Kawase, T.; Kurata, H. *Chem. Rev.* **2006**, *106*, 5250–5273. (e) Hirsch, A. *Phys. Stat. Sol. B* **2006**, *243*, 3209–3212. (f) Tagmatarchis, N.; Prato, M. *Pure Appl. Chem.* **2005**, *77*, 1675–1684. (g) Sanchez, L.; Martin, N.; Guldi, D. M. *Angew. Chem., Int. Ed.* **2005**, *44*, 5374–5382. (h) D'Souza, F.; Ito, O. *Coord. Chem. Rev.* **2005**, *249*, 1410–1422. (i) Konishi, T.; Ikeda, A.; Shinkai, S. *Tetrahedron* **2005**, *61*, 4881–4899.

(2) Collings, A. F.; Critchley, C. *Artificial Photosynthesis: From Basic Biology to Industrial Application*; Wiley-VCH: Weinheim, Germany, 2005.

(3) Guldi, D. M.; Illescas, B. M.; Atienza, C. M.; Wielopolski, M.; Martín, N. *Chem. Soc. Rev.* **2009**, *38*, 1587–1597.

(4) (a) *Endofullerenes: A New Family of Carbon Clusters*; Akasaka, T., Nagase, S., Eds.; Kluwer: Dordrecht, The Netherlands, 2002. (b) Nagase, S.; Kobayashi, K.; Akasaka, T.; Wakahara, T.; In *Fullerenes: Chemistry, Physics and Technology*; Kadish, K., Ruoff, R. S., Eds.; John Wiley & Sons: New York, 2000; pp 231−251. (c) Naydenov, B.; Spudat, C.; Harneit, W.; Süss, H. I.; Hulliger, J.; Nuss, J.; Jansen, M. *Chem. Phys. Lett.* **2006**, *424*, 327–332.

(5) (a) Akasaka, T.; Kato, T.; Kobayashi, K.; Nagase, S.; Yamamoto, K.; Funasaka, H.; Takahashi, T. *Nature* **1995**, *374*, 600–601. (b) Koltover, V. K.; Logan, J. W.; Heise, H.; Bubnov, V. P.; Estrin, Y. I.; Kareev, I. I.; Lodygina, V. P.; Pines, A. *J. Phys. Chem. B* **2004**, *108*, 12450–12455. (c) Koltover, V. K.; Bubnov, V. P.; Estrin, Y. I.; Lodygina, V. P.; Davydov, R. M.; Subramoni, M.; Manoharan, P. T. *Phys. Chem. Chem. Phys.* **2003**, *5*, 2774–2777.

(6) (a) Tsuchiya, T.; Sato, K.; Kurihara, H.; Wakahara, T.; Maeda, Y.; Akasaka, T.; Ohkubo, K.; Fukuzumi, S.; Kato, T.; Nagase, S. *J. Am. Chem. Soc.* **2006**, *128*, 14418–14419. (b) Tsuchiya, T.; Sato, K.; Kurihara, H.; Wakahara, T.; Nakahodo, T.; Maeda, Y.; Akasaka, T.; Ohkubo, K.; Fukuzumi, S.; Kato, T.; Mizorogi, N.; Kobayashi, K.; Nagase, S. *J. Am. Chem. Soc.* **2006**, *128*, 6699–6703. (c) Tsuchiya, T.; Kurihara, H.; Sato, K.; Wakahara, T.; Akasaka, T.; Shimizu, T.; Kamigata, N.; Mizorogi, N.; Nagase, S. *Chem. Commun.* **2006**, 3585–3587.

(7) (a) Pinzón, J. R.; Plonska-Brzezinska, M. E.; Cardona, C. M.; Athans, A. J.; Sankaranarayanan, S. G.; Guldi, D. M.; Herranz, M. Á.; Martín, N.; Torres, T.; Echegoyen, L. *Angew. Chem., Int Ed.* **2008**, *47*, 4173–4176.

(8) Ross, R. B.; Cardona, C. M.; Guldi, D. M.; Sankaranarayanan, S. G.; Reese, M. O.; Kopidakis, N.; Peet, J.; Walker, B.; Bazan, G. C.; Keuren, E. V.; Holloway, B. C.; Drees, M. *Nat. Chem.* **2009**, *8*, 208–212.

(9) Takano, Y.; Herranz, M. Á.; Martín, N.; Sankaranarayanan, S. G.; Guldi, D. M.; Tsuchiya, T.; Nagase, S.; Akasaka, T. *J. Am. Chem. Soc.* **2010**, *132*, 8048–8055.

(10) Guldi, D. M.; Feng, L.; Sankaranarayanan, S. G.; Nikawa, H.; Yamada, M.; Mizorogi, N.; Tsuchiya, T.; Akasaka, T.; Nagase, S.; Herranz, M. Á.; Martín, N. *J. Am. Chem. Soc.* **2010**, *132*, 9078–9086.

(11) Tsuchiya, T.; Wakahara, T.; Shirakura, S.; Maeda, Y.; Akasaka, T.; Kobayashi, K.; Nagase, S.; Kato, T.; Kadish, K. M. *Chem. Mater.* **2004**, *16*, 4343–4346.

(12) Ito, O. *Res. Chem. Intermed.* **1997**, *23*, 389–402.

(13) See Supporting Information.

(14) Kato, T. *J. Mol. Struct.* **2007**, *838*, 84–88.

(15) Reduction potentials of $Sc_3N@C_{80}$ and C_{60} in nitrobenzene are −1.07 and −0.96 V vs Fc/Fc^+, respectively.

(16) Reduction potential of $La_2@C_{80}$ is −0.16 V vs Fc/Fc^+.